Genome-Wide Mapping of Histone Modifications in Two Species of Leptosphaeria Maculans Showing Contrasting Genomic Organization and Host Specialization

Jessica Louise Soyer (jessica.soyer@inrae.fr)
INRAE Île-de-France-Versailles-Grignon: Institut National de Recherche pour l'Agriculture l'Alimentation et l'Environnement Centre Ile-de-France-Versailles-Grignon https://orcid.org/0000-0002-9424-1053

Colin Clairet
INRAE Île-de-France-Versailles-Grignon: Institut National de Recherche pour l'Agriculture l'Alimentation et l'Environnement Centre Ile-de-France-Versailles-Grignon

Elise J. Gay
INRAE Île-de-France-Versailles-Grignon: Institut National de Recherche pour l'Agriculture l'Alimentation et l'Environnement Centre Ile-de-France-Versailles-Grignon

Nicolas Lapalu
INRAE Île-de-France-Versailles-Grignon: Institut National de Recherche pour l'Agriculture l'Alimentation et l'Environnement Centre Ile-de-France-Versailles-Grignon

Thierry Rouxel
INRAE Île-de-France-Versailles-Grignon: Institut National de Recherche pour l'Agriculture l'Alimentation et l'Environnement Centre Ile-de-France-Versailles-Grignon

Eva H. Stukenbrock
Max Planck Institute for Evolutionary Biology: Max-Planck-Institut fur Evolutionsbiologie

Isabelle Fudal
INRAE Île-de-France-Versailles-Grignon: Institut National de Recherche pour l'Agriculture l'Alimentation et l'Environnement Centre Ile-de-France-Versailles-Grignon

---

Research

Keywords: Leptosphaeria maculans, ChIP-seq, RNA-seq, comparative epigenomics, chromatin, heterochromatin, effectors, host-pathogen interaction

Posted Date: September 18th, 2020

DOI: https://doi.org/10.21203/rs.3.rs-73550/v1

Genome-wide mapping of histone modifications in two species of *Leptosphaeria maculans* showing contrasting genomic organization and host specialization

Jessica L. Soyer[1,2,#], Colin Clairet[1], Elise J. Gay[1], Nicolas Lapalu[1], Thierry Rouxel[1], Eva H. Stukenbrock[2,¥], Isabelle Fudal[1,¥]

[1]Université Paris-Saclay, INRAE, AgroParisTech, UMR BIOGER, 78850, Thiverval-Grignon, France

[2]Max Planck Institute for Evolutionary Biology, August-Thienemann-Str. 2, 24306 Plön, and Christian-Albrechts University of Kiel, Am Botanischen Garten 1-9, 24118 Kiel, Germany

[¥]Co-last authors

[#]Corresponding author: J.L. Soyer; jessica.soyer@inrae.fr

Word count

Abstract: 246; Introduction: 1080; Materials and Methods: 991; Results: 2319; Discussion: 1843

Keywords

Leptosphaeria maculans, ChIP-seq, RNA-seq, comparative epigenomics, chromatin, heterochromatin, effectors, host-pathogen interaction.

ABSTRACT

Background: In plant-associated fungi, the epigenome is increasingly recognized as an important regulator of the expression of genes involved in interaction with the host plant. *Leptosphaeria maculans* 'brassicae' (Lmb) and *Leptosphaeria maculans* 'lepidii' (Lml) are closely-related phytopathogenic species that exhibit a large macrosynteny but contrasting genome structure. Lmb has more than 30% of repeats clustered in large repeat-rich regions, while the Lml genome has only a small amount of evenly distributed repeats. Repeat-rich regions of Lmb are enriched in effector genes, expressed during plant infection. The distinct genome structures of Lmb and Lml provide an excellent model for comparing the organization of pathogenicity genes in relation to the chromatin landscape in two closely related phytopathogenic fungi. Here, we performed chromatin immunoprecipitation (ChIP) during axenic culture, targeting histone modifications typical for heterochromatin or euchromatin, combined with transcriptomic analysis to analyse the influence of chromatin organisation on gene expression.

Results: In both species, we found that facultative heterochromatin are enriched with genes lacking functional annotation, including numerous effector and species-specific genes. Notably, orthologous genes located in H3K27me3-domains are enriched with effector genes. Compared to other fungal species, including Lml, Lmb is distinct in having large H3K9me3-domains associated with repeat-rich regions that contain numerous species-specific effector genes.

Conclusion: Discovery of these two distinctive heterochromatin landscapes now raises questions about their involvement in the regulation of pathogenicity, the dynamics of these domains during plant infection, and the selective advantage to the fungus to host effector genes in H3K9me3- or H3K27me3-domains.

Background

Each year, hundreds of millions of tons of agricultural crops are devastated by plant pathogenic fungi or made unfit for consumption due to contamination by mycotoxins (1). Management strategies to control fungal infection mainly involve chemical control or breeding for naturally resistant crop cultivars. However, fungal plant pathogens have proven capable of rapidly evolving resistance against fungicides (1) and to overcome specific plant resistance genes within a few years (for instance in *Leptosphaeria maculans*; 2), emphasising the need for improved control methods.

Understanding the determinants of the extreme adaptive abilities of fungal plant pathogens is a critical issue for the development of effective and sustainable control methods. In that respect, comparative and population genomic analyses have provided new insights into the evolutionary dynamics of fungal plant pathogens (e.g. 3-5). Notably, transposable elements (TE) have been shown to play a crucial role in shaping the genome structure of plant-pathogenic fungi. TEs are often organized in clusters, compartmentalizing the genome into gene-rich regions and TE-rich regions (e.g. in *L. maculans* and in *Mycosphaerella fijiensis*; 4, 6, 7). While the gene density in TE-rich regions is low, genes located in these regions have been shown to evolve faster than genes located in TE-poor regions (8, 9). Interestingly, rapidly evolving genes in TE-rich regions have, in many cases, been identified as genes involved in niche adaptation and notably effector genes. Effectors are considered as key elements of pathogenesis, allowing pathogens to circumvent host recognition, impede defence reactions and facilitate host invasion. Effectors are mainly secreted proteins, but can also correspond to secondary metabolites and small RNAs (10, 11,

12). Plants have evolved strategies to recognize and counteract effectors, exposing them to a strong selection pressure by the host immune system (2, 13, 14). Indeed, in the course of the co-evolution between a pathogen and its host, the host has developed an active immune system allowing the direct or indirect recognition of some effector molecules, to activate defence responses, often involving a local cell death, called the hypersensitive response. Effectors that can be recognized by the host are called avirulence proteins (10, 15).

Leptosphaeria maculans 'brassicae' (hereinafter referred to as Lmb) belongs to the Dothideomycete class of Ascomycete fungi and is responsible for causing stem canker of oilseed rape (*Brassica napus*). Lmb displays a complex, hemibiotrophic life cycle, during which it alternates between different nutritional modes on its host plant. It causes necrosis on different plant organs: leaves, more rarely seedpods, and the base of the stem, causing lodging of the plant and yield losses (16). The most efficient method of disease control relies on the use of major resistance genes present in oilseed rape and other Brassica species. Although efficient, this control method is not sustainable, as Lmb is able to "break down" novel sources of genetic resistance rapidly (2). One third of the Lmb genome is made of TE-rich regions. These regions are enriched with putative effector genes and include all currently known avirulence genes. These avirulence genes are highly expressed in the first seven days of leaf and cotyledon infection (17-26). Another set of putative proteinaceous effector genes are located in gene-rich regions of the genome and are specifically expressed during stem infection (27).

In eukaryotic cells, chromatin can adopt different conformational states directly influencing gene expression: gene-rich euchromatin, sheltering constitutively expressed genes, and gene-poor heterochromatin, in which genes are silent. The different chromatin states are characterized by

84 different post-translational modifications of histones around which DNA is wrapped. Typically,
85 heterochromatin is enriched in the trimethylation of the lysine 9 of histone H3 (H3K9me3) and
86 lysine 27 (H3K27me3) while euchromatin is enriched in the di- (or tri-) methylation of the lysine
87 4 of histone H3 (H3K4me2) (28). Recent research has focused on dynamic changes in DNA
88 accessibility and how these may play fundamental roles in the adaptation of different individuals
89 to abiotic and biotic stresses (29, 30). In fungal plant pathogens or endophytes, evidence is
90 accumulating that transcriptional reprogramming of effector genes (either proteinaceous or
91 metabolic) is tightly controlled by chromatin-based regulatory mechanisms (for example in
92 *Fusarium graminearum*, *Epichloe festucae*, Lmb and *Zymoseptoria tritici*; 31-35). In Lmb, the
93 location of avirulence genes in TE-rich regions has an influence on their evolution under
94 selection pressure (6, 36) and plays a role in regulating their expression during axenic culture via
95 deposition of H3K9me3 (33).
96 Lmb belongs to the *L. maculans* / *Leptosphaeria biglobosa* species complex, comprising species
97 with different host specialization and genome organization (4). Within the species complex, the
98 *L. maculans* species infecting oilseed rape, Lmb, is the only one having large regions of its
99 genome enriched with TEs while other genomes have a low TE-content (~3-15% compared to
100 more than 30% TEs in Lmb; 4, 6, 37). For example, the genome of the species that is most closely
101 related to Lmb, *Leptosphaeria maculans* 'lepidii' (hereinafter referred to as Lml), which infects
102 crucifers such as *Lepidium sativum*, and to a lesser extent *Camelina sativa* and *Brassica rapa*
103 (38), has a low TE content (3% of TEs; 4). Interestingly, the genomes of Lmb and Lml show a high
104 level of macrosynteny, with only a few intra-chromosomal inversions, but differ in their TE
105 content with Lmb having undergone a massive TE expansion 5 million years ago corresponding

to the speciation date (4). Invasion of TEs in the genome of Lmb has shaped its genome, with alternating TE-rich regions and gene-rich regions. In contrast, the Lml genome shows a homogeneous TE distribution along the chromosomes (4).

The distinct genome organisation shown by Lmb and Lml thus provides us with a model of choice for comparing epigenomic organization in two closely related phytopathogenic fungi, to determine the genomic location of pathogenicity/effector genes in relation to the chromatin landscape and the influence of chromatin structure on gene expression. Comparative epigenomic analyses, at the intra- or inter-species levels, are very sparse and this remains an underexplored field of study, at least in fungi (39, 40). We present here the first comparative epigenomic analysis of both euchromatin and heterochromatin marks in two closely related phytopathogenic fungi. We first performed ChIP-seq and RNA-seq during axenic culture to compare the distribution of three histone modifications, H3K4me2, H3K9me3 and H3K27me3, and then investigated whether chromatin organization is conserved between Lmb and Lml by assessing whether orthologous genes, and pathogenicity-related genes, are located in similar chromatin domains in each species. Lastly, we assessed the influence of the chromatin landscape on gene expression during axenic growth, focusing mostly on pathogenicity related genes that may be species-specific.

Methods

Fungal isolates

The isolate v23.1.3 of *L. maculans* 'brassicae' and the isolate IBCN84 of *L. maculans* 'lepidii' were used throughout the analyses (Rouxel *et al.,* 2011; Grandaubert *et al.,* 2014). Fungal cultures

were maintained as described previously (41). For chromatin immunoprecipitation and transcriptomic analyses performed during *in vitro* growth, mycelium of Lmb and Lml were grown on V8 agar medium at 25°C for seven days. Then 10 plugs of mycelium were inoculated into 100 ml of Fries liquid medium in Roux bottle. Mycelia were harvested after growing for 7 days at 25°C, filtered and washed thoroughly with distilled water, and immediately placed in liquid nitrogen until further used. ChIP experiments were performed on fresh material.

Chromatin immunoprecipitation and high-throughput sequencing

ChIP was performed from freshly-harvested mycelium grown in Fries liquid culture, as described in Soyer *et al*. (42), with minor modifications. ChIP was performed on native material (without crosslinking) using antibodies targeting histone modifications H3K4me2 (Merck ref. 07-030), H3K9me3 (Active Motif, Carlsbad, CA, USA; ref. 39161), or H3K27me3 (Active Motif, Carlsbad, CA, USA; ref. 39155). Three different ChIPs (i.e. three biological replicates) were performed for each of the histone modifications. Libraries were prepared from all biological replicates, individually, according to the Illumina TruSeq protocol "Ultra Low Input DNA library". Libraries were sequenced with an Illumina HiSeq 2000 genome analyzer at the Max Planck Genome centre Cologne, Germany (https://mpgc.mpipz.mpg.de/home/). Sequencing data are available under the GEO accession number GSE150127.

Analysis of ChIP-seq data and identification of significantly enriched domains

Analysis of ChIP-seq datasets was performed as described in Schotanus *et al*. (43). Quality of Illumina reads was analysed using FastQC

150 (https://www.bioinformatics.babraham.ac.uk/projects/fastqc/). Based on results of this analysis,
151 ten bp were trimmed from the 5' end. Processed reads were mapped on the reference genome
152 of Lmb (37) or Lml (4) using Bowtie2 (44) with default parameters (Additional table 1). Peak
153 calling analysis was performed on each ChIP sequencing dataset, to identify significantly
154 enriched domains for either H3K4me2, H3K9me3 or H3K27me3, using RSEG (45). A domain was
155 considered if identified in at least two out of the three biological replicates. The Integrative
156 Genome Viewer (46) was used to visualize location of each domain along genomes of Lmb and
157 Lml according to other genome features (gene annotation, TE-annotation, GC-content).
158 Coverage of the histone modifications was assessed in 10 kb non-overlapping sliding windows
159 along the supercontigs and correlation analyses, using Kendall's *T* correlation coefficient, were
160 performed between biological replicates to check for reproducibility (Additional tables 2 and 3).
161 In order to assess significant enrichment of H3K4me2, H3K9me3 or H3K27me3 in certain
162 categories of genes (such as proteinaceous or metabolic effector-encoding genes), a Chi^2 test
163 was applied to compare the expected proportion of a given category of genes across the entire
164 genome to the observed distribution of the gene category in H3K4me2-, H3K9me3- or
165 H3K27me3-domains (35). Enrichment was considered significant with a *P value* < 0.01; analyses
166 were done using R, version 3.0.2 (www.r-project.org).
167
168 RNA extraction, RNA-sequencing and expression analysis
169 Total RNA was extracted from mycelium grown for one week in Fries liquid medium as previously
170 described (18). The NEBNext Ultra Directional RNA Library Prep Kit for Illumina (cat. # E7420L
171 New England BioLabs) was used to prepare RNA-seq libraries and sequencing was performed on

a HiSeq 4000 Illumina genome analyser using 50 paired-end reads. Raw reads were then pre-processed with Trimmomatic (47) to remove short reads (<30 bp) and eliminate sequencing adaptors. Cleaned reads were then mapped against each genome using STAR with default parameters (48; Additional table 1). Gene expression was evaluated using the rpkm_count function of EdgeR (49). Genes with RPKM ≥ 2 were considered expressed. Sequencing data are available under the GEO accession number GSE150127.

Identification of orthologues and annotation of genes encoding proteinaceous effectors in Lmb and Lml

The genome of Lmb encodes 13,047 proteins and that of Lml 11,272 proteins (4, 37). Orthologous proteins between Lmb and Lml were identified using OrthoFinder with default parameters (50).

Based on the new assembly and annotation available for the genome of Lmb (37), an updated repertoire of putative proteinaceous effector genes (encoding Small Secreted Proteins, SSP) has been predicted. Therefore, to compare effector repertoires of Lmb and Lml, the same pipeline for the prediction of putative effector genes was applied to both species. Signal peptide and subcellular localization were predicted by SignalP version 4.1 (51) and TargetP version 1.1 (52) respectively. Transmembrane domains were predicted by TMHMM version 2.0. The predicted secretome contained all proteins with no more than one transmembrane domain and either a predicted signal peptide or a predicted extracellular localization. The final effector repertoires were created by applying a size cut-off of 300 amino acids on the predicted secretome. In parallel, EffectorP version 1.0 (53) was used on the predicted secretome and, for Lml, four

194 proteins were predicted as effectors with a size higher than 300 amino acids. These four proteins
195 were added to the SSP set. This predicted a repertoire of 1,080 and 892 SSP-encoding genes for
196 Lmb and for Lml, respectively.
197
198 Analysis of GO enrichment
199 Gene Ontology (GO) annotations of the Lmb and Lml genes were retrieved from Dutreux *et al*.
200 (37) and Grandaubert *et al*. (4) respectively. GO term enrichment analysis of the H3K4me2-,
201 H3K9me3- and H3K27me3-associated genes was performed with the plug-in Biological networks
202 Gene ontology (BinGo; v3.0.3) of the cytoscape software (54). List of genes submitted to BINGO
203 were considered as significantly enriched for a given GO term with an associated False Discovery
204 Rate (FDR) ≤ 0.01 for the biological processes.
205 A Chi² test, or a Fisher's exact test for small sized-population, were applied to identify significant
206 enrichment of H3K4me2-, H3K9me3- or H3K27me3-domains for certain categories of genes: the
207 expected proportion of a given category of genes across the entire genomes of Lmb or Lml was
208 compared to the observed distribution of the gene category in the H3K4me2-, H3K9me3- or
209 H3K27me3-domains. Enrichment was considered significant with a *P value* < 0.01. All analyses
210 were done using R, version 3.0.2 (www.r-project.org).
211
212 **Results**
213 A different genome organisation but similar epigenomic properties in both genomes
214 To assess the genome-wide distribution of histone marks in Lmb and Lml during axenic growth,
215 we performed ChIP-seq experiments using antibodies against histone modifications H3K4me2,

H3K9me3 and H3K27me3 (Additional table 1). Mapping of the ChIP-seq data was followed by identification of significantly enriched domains, for any of the histone modifications targeted, and reproducibility of the biological replicates was assessed (Additional tables 2 and 3). Based on the genomic coordinates of the H3K4me2-, H3K9me3- and H3K27me3-domains, the number of bases associated with any of the three histone modifications was evaluated, for each genome, in 10 kb sliding-windows. In the genomes of Lmb and Lml, the proportion of H3K4me2 and H3K27me3 was similar (H3K4me2: 39% in Lmb vs. 32% in Lml; H3K27me3: 19% in Lmb vs. 13% in Lml) while the proportion of H3K9me3 was strikingly different (33% and 4% for Lmb and Lml, respectively) (Additional tables 4 and 5). While the median size of the H3K4me2- and H3K27me3-domains was similar in both genomes, the Lmb genome displayed extremely large H3K9me3-domains, with a domain encompassing up to 230 kb, while the maximum size of the H3K9me3-domains in Lml was only 12 kb (Figures 1; 2).

In the genomes of Lmb and Lml, H3K4me2- and H3K9me3-domains were mutually exclusive (Kendall's *T*: -0.57 and -0.16, $P < 2.2.10^{-16}$ for Lmb and Lml respectively; Figure 2; Additional figure 1; Tables 1 and 2). We identified a positive correlation between the location of TEs and H3K9me3-domains (Kendall's *T*: 0.87 and 0.68, $P < 2.2.10^{-16}$ for Lmb and Lml respectively; Figure 2; Figure 3A, 3C; Figure S1; Tables 1 and 2) and between the location of coding sequences (CDS) and H3K4me2 (Kendall's *T*: 0.55 and 0.25, $P < 2.2.10^{-16}$ for Lmb and Lml respectively; Figure 2; Figure S1; Figure 3A, 3C; Tables 1 and 2). In the genome of Lmb, a weak correlation was demonstrated between CDS and H3K27me3-domains (Kendall's *T*: 0.12, $P < 2.2.10^{-16}$; Figure S1; Tables 1, 2). For Lmb and Lml, the coverage of H3K9me3 and H3K27me3 was not homogeneous across all SCs because some are >2-fold more highly enriched with these histone modifications

238 compared to others. An extreme example of this situation was identified on the dispensable
239 chromosome of Lmb (6, 55), which is extremely enriched in TEs compared to the rest of the
240 genome (35% of TEs in the core genome and 93% of TEs in the dispensable chromosome).
241 Consistently, a strong enrichment in H3K9me3 was observed in the dispensable chromosome
242 (32% in the core genome and 90% in the dispensable chromosome), with only a few H3K4me2-
243 and H3K27me3-domains (Figure 3A and 3B). In Lmb, we found that many sub-telomeric regions
244 showed overlaps between H3K9me3 and H3K27me3, whereas these marks did not overlap on
245 the chromosome arms, even within large TE-rich regions (Figure 2). The assembly quality of the
246 Lml genome was not sufficient to allow us to evaluate whether this was a common feature
247 between the two species.
248

Table 1. Correlation between transposable elements, coding sequences and histone modifications in the *L. maculans* 'brassicae' genome.

	CDS	TE	H3K4me2	H3K9me3	H3K27me3
CDS	1	-0.63	0.55	-0.60	0.12
TE	-0.63	1	-0.58	0.87	-0.25
H3K4me2	0.55	-0.58	1	-0.57	-0.11
H3K9me3	-0.60	0.87	-0.57	1	-0.24
H3K27me3	0.12	-0.25	-0.11	-0.24	1

The coverage of transposable elements (TE), coding sequences (CDS) and histone modifications (H3K9me3, H3K27me3, H3K4me2) along the genome of *L. maculans* 'brassicae' was analysed in 1000 bp sliding windows. A Kendall's *T* correlation analysis was done using R.

Table 2. Correlation between transposable elements, coding sequences and histone modifications in the *L. maculans* 'lepidii' genome.

	CDS	TE	H3K4me2	H3K9me3	H3K27me3
CDS	1.00	-0.22	0.25	-0.25	-0.05
TE	-0.22	1.00	-0.16	0.68	0.00
H3K4me2	0.25	-0.16	1.00	-0.16	-0.23
H3K9me3	-0.25	0.68	-0.16	1.00	0.01
H3K27me3	-0.05	0.00	-0.23	0.01	1.00

The coverage of transposable elements (TE), coding sequences (CDS) and histone modifications (H3K9me3, H3K27me3, H3K4me2) along the genome of *L. maculans* 'lepidii' was analysed in 1000 bp sliding windows. A Kendall's *T* correlation analysis was done using R.

249

250 H3K4me2-domains associate with genes involved in primary metabolism while H3K27me3-

251 domains shelter genes involved in niche adaptation and cell wall degradation

252 Genes associated with H3K4me2-, H3K9me3- or H3K27me3-domains were identified in the

253 genomes of Lmb and Lml during axenic growth. Overall, the number of genes associated with

254 any of the histone post-translational modifications was similar in both species, with more than

255 50% of the predicted genes associated with H3K4me2, ~14% of the genes associated with

256 H3K27me3 and only a few genes associated with H3K9me3 (104 and 70 respectively in Lmb and

257 Lml; Figure 4). In Lmb, there was a higher number of genes associated with both H3K4me2 and

258 H3K27me3 than in Lml (2,044 and 361 for Lmb and Lml, respectively) (Figure 4). In both

259 genomes, a GO annotation could be assigned to 30-40% of the predicted genes (5,076 and 3,725

260 genes for Lmb and Lml, respectively; 4, 37). Euchromatin was enriched with genes with a GO

261 annotation (X^2 test, $P < 2.2.10^{-16}$) because more than 40% of the genes associated with H3K4me2

262 had a GO annotation (3,276 and 2,581 genes for Lmb and Lml respectively). Between 20 and

28% of the genes associated with H3K27me3 (572 and 288 genes for Lmb and Lml, respectively) had a GO annotation. However, none of the genes located in H3K9me3-domains, H3K9/K27me3-domains or H3K4me2/H3K27me3-domains had a GO annotation. In other words, genes located in heterochromatin were enriched with genes lacking any functional annotation (X^2 test, $P < 2.2.10^{-16}$). For both species, genes associated with H3K4me2 displayed a wide variety of annotated functions corresponding to primary metabolism and basic cellular functions, such as translation (GO:0006412; 206 genes) or cellular protein metabolic process (Additional tables 6, 7). For both species, only a few GO terms were identified among genes associated with H3K27me3. Nevertheless, in Lmb these genes were significantly enriched in GO terms associated with carbohydrate metabolic process (GO:0005975; 82 genes), oxydo-reduction process (GO:0055114; 149 genes) and transmembrane transport (GO:0055085; 104 genes) ($P \leq 0.01$) (Additional table 8). As for Lml, probably due to the lower number of genes associated to H3K27me3, only a few GO annotation enrichments were detected. Only one GO enrichment was found in common with Lmb, namely carbohydrate metabolic process (GO:0005975; 41 genes). Other enrichments corresponded to a few genes classified as response to chemical (GO: 42221; 20 genes), response to nitrogen compound (GO:1901698; 10 genes), response to organophosphorus (GO: 46683, 10 genes) and others (Additional table 9). Although most GO enrichments found among sets of genes associated with H3K27me3 in Lmb and Lml did not overlap, both types of enrichments suggest that H3K27me3-associated genes might be involved in stress response mechanisms, but may also be involved in feeding or cell wall degradation processes during plant infection.

H3K4me2-domains are associated with expressed genes while H3K9me3- and H3K27me3-domains are associated with silent genes during axenic growth

We performed a genome-wide transcriptomic analysis of fungal cultures grown *in vitro*, and we correlated gene expression patterns with the distribution of histone modifications. In Lmb, 10,934 genes (83% of the predicted genes) and 7,735 genes in Lml (69% of the predicted genes) were expressed during vegetative growth. Considering the top 100 most expressed genes of Lmb, 68 were associated with H3K4me2 while two were located within a H3K27me3-domain and none in a H3K9me3-domain (data not shown). In Lml, 71 were located within a H3K4me2-domain while five were located in a H3K27me3-domain (data not shown). These data were confirmed at a genome-wide scale because H3K4me2-domains were enriched with genes expressed during axenic culture (7,104 of the genes associated with H3K4me2 were expressed in Lmb and 5,338 in Lml; Figure 5; $P < 2.2.10^{-16}$). On the contrary, H3K9me3- and H3K27me3-domains were enriched with genes that were silent during *in vitro* growth (Figure 5; $P < 2.2.10^{-16}$). On the other hand, in both species, genes that were associated with both H3K4me2 and H3K27me3 were expressed during axenic growth (90% and 87% of the genes, respectively, in Lmb and Lml) and their level of expression was similar to that of genes located in H3K4me2-domains (Figure 5).

In both species, this transcriptomic analysis confirmed that genes located in a H3K4me2-domain were more likely to be expressed while those located in H3K9me3- and H3K27me3-domains were more likely to be silent.

307 Heterochromatin domains are enriched with species-specific genes

308 A total of 7,393 genes were conserved between both species. H3K4me2-domains were enriched
309 with genes conserved between these two species, for example 4,892 Lmb genes located in
310 euchromatin regions during growth *in vitro* were conserved (X^2 test, $P < 2.2.10^{-16}$) and the vast
311 majority of these (4,298, i.e. 88%) were expressed during axenic growth in both Lmb and Lml.
312 Most of the conserved genes associated with H3K4me2 were involved in primary metabolism as
313 mentioned above. Genes associated with both H3K4me2 and H3K27me3 were also enriched
314 with conserved genes (1,318 and 262 genes, respectively, in Lmb and Lml) representing more
315 than 65% of the genes in these domains (X^2 test, $P < 5.2.10^{-3}$). Two genes involved in
316 heterochromatin assembly and maintenance were analysed previously through gene silencing
317 (*LmHP1* and *LmKMT1*/*DIM5*; 33). *LmHP1* is conserved in Lml and located in euchromatin in both
318 species. *LmKMT1* is also conserved in both species, being located in a H3K4me2/H3K27me3
319 domain in Lmb and within a H3K4me2/H3K9me3 domain in the case of Lml, during axenic
320 growth. In contrast, H3K27me3- and H3K9me3-domains were significantly enriched with
321 species-specific genes (a total of 865 genes and 661 genes, respectively, in Lmb and Lml; X^2 test,
322 $P < 2.2.10^{-16}$). Among genes located in heterochromatin in both species (either H3K9me3-,
323 H3K27me3- or H3K9/K27me3-domains), 445 were conserved between Lmb and Lml; of which 83
324 were expressed and 182 were repressed during axenic growth in both species. No GO
325 enrichment was found for these genes and predicted functions were sparse, with less than 45%
326 of them having a functional annotation. Strikingly, the main enrichment was in genes encoding
327 putative effectors (16% of the genes).
328

329 Heterochromatin domains are enriched with proteinaceous and metabolic effector genes

330 We then focused on candidate proteinaceous or metabolic effectors and wondered whether
331 they were conserved and showed a distinct pattern of histone modifications. In the genome of
332 Lmb, 2,478 genes (i.e. 12% of the total genes) were associated with TE-rich regions (i.e. located
333 within 2 kb distance of a TE sequence), of which 289 genes encoded putative proteinaceous
334 effectors. Hence, although a new prediction of the effector repertoire was performed here,
335 based on the new assembly of the Lmb genome, TE-rich regions were significantly enriched with
336 proteinaceous effector genes, as was already shown by Rouxel *et al*. (6; X^2 test, $P = 9.6.10^{-16}$).
337 Similarly, both H3K9me3- and H3K27me3-associated genes were significantly enriched with
338 putative proteinaceous effectors, as they represented, respectively, 36% and 14% of the genes
339 associated with these histone modifications *in vitro* (X^2 test, $P < 2.2.10^{-16}$; Table 3). Likewise, in
340 Lml, TE-rich regions, H3K9me3- and H3K27me3-domains were significantly enriched with
341 putative proteinaceous effector genes while H3K4me2-domains were significantly depleted in
342 such genes compared to the rest of the genome (Table 3). Among the 1,080 putative
343 proteinaceous effector genes predicted in Lmb (8.2% of the total predicted genes) and the 892
344 putative effector genes of Lml (7.9% of the total predicted genes), 274 were conserved between
345 both species. Hence, more than two-thirds of the effector repertoire is species-specific (X^2 test, P
346 $< 2.2.10^{-16}$), confirming our previous findings (4). Overall, orthologous effector-encoding genes
347 were associated with the same types of chromatin domains in Lmb and Lml. For example, 98% of
348 the Lmb effector genes located in a euchromatin environment were also associated with
349 H3K4me2 in Lml (82% of Lml effector genes located in euchromatin regions were also associated
350 with H3K4me2 in Lmb). H3K27me3- and H3K9me3-domains were enriched with species-specific

351 effector genes in both species (Table 3). As a striking example of the non-random location of
352 effector genes in the two genomes, and the enrichment of heterochromatin regions with
353 species-specific effectors, all nine currently known avirulence genes of Lmb were located in
354 H3K9me3-domains *in vitro*, consistent with the fact that these genes are located in TE-rich
355 genomic compartments; none of the nine was conserved in the genome of Lml. Twenty-eight
356 other proteinaceous effector-encoding genes were located in TE-rich, H3K9me3-domains in Lmb,
357 and only one of them had a putative ortholog in Lml. The 274 orthologous genes encoding
358 effectors were then investigated for their distribution in euchromatic/heterochromatic regions
359 during vegetative growth and for conservation of their location between orthologs. There was
360 no obvious bias in the distribution of chromatin marks among the 274 genes, which is
361 comparable to the overall distribution of marks among all genes of the effector repertoires (data
362 not shown). At the individual gene level, 86 of the 274 orthologs were located in a similar
363 chromatin domain in Lmb and Lml, including 83 genes associated with H3K4me2 and 47 genes
364 associated with H3K27me3 in both genomes. In contrast to avirulence genes, 'late' putative
365 effector-genes of Lmb (i.e. expressed during stem colonization) were located outside of TE-rich
366 regions (27). Three of the 11 experimentally validated 'late' effector genes were located in a
367 H3K4me2-domain while others were located in a H3K9me3- (two cases), a H3K27me3- (three
368 cases), a H3K9/K27me3- (one case) or a H3K4me2/K27me3-domain (two cases), suggesting that
369 'late' effector genes were also enriched with heterochromatin domains during growth *in vitro*.
370 Interestingly, and contrary to the trend observed for Lmb avirulence effector genes (and other
371 effector candidates associated with TE-rich regions), only two of the 11 'late' putative effector
372 genes, either located in H3K9me3- or H3K27me3-domains, were not conserved in Lml. Taken

373 together, these data show that, independently of the species or the stage at which they are
374 expressed during infection, proteinaceous effector genes are enriched in H3K9me3- or
375 H3K27me3-domains during axenic growth.
376 The genomes of Lmb and Lml contain secondary metabolite gene clusters including key genes
377 encoding PKS (Polyketide Synthases) and NRPS (Non-Ribosomal Peptide Synthetases). Twenty-
378 seven such genes were predicted in Lmb among which 24 were conserved in Lml, but they were
379 overall absent from other closely related species (4, 6; Additional table 10). Of these, only three
380 have been experimentally demonstrated to be involved in Lmb pathogenicity, namely the PKS
381 responsible for synthesis of abscisic acid (ABA), only expressed during cotyledon infection (56),
382 the PKS responsible for producing phomenoic acid (57), and the NRPS responsible for
383 synthetising sirodesmin, a toxin produced during stem infection (58, 59). The ABA PKS and all
384 seven genes of the cluster, which are intermingled with three TE-rich regions, were entirely
385 absent from the genome of Lml, while the other two were conserved (Additional table 10). In
386 Lmb, 81% of the PKS/NRPS-encoding genes were associated to H3K27me3- or
387 H3K4me2/H3K27me3-domains (22 PKS/NRPS; Fisher's exact test, $P = 1.3.10^{-7}$). Likewise in the Lml
388 genome, H3K27me3-domains were enriched with PKS/NRPS-encoding genes (12 PKS/NRPS;
389 Fisher's exact test, $P = 1.7.10^{-4}$), and all of them had orthologs associated with similar marks in
390 Lmb. The similar chromatin context also resulted in similar regulation in most of the cases, with
391 19 of the orthologs being similarly expressed during *in vitro* growth (17 expressed and two
392 repressed; Additional table 10).
393
394 **Discussion**

The sister species *L. maculans* 'brassicae' and *L. maculans* 'lepidii' exhibit marked differences in their genome organisation. Notably, Lmb has large TE-rich domains structuring the genome into alternating gene-rich and TE-rich regions (6). In the genome of Lml, in contrast, TEs are evenly distributed across the genome and no compartmentalisation of the genome is evident in relation to TE location (4). The massive invasion of the Lmb genome by TEs occurred ca. 5 MYA and was postulated to have been instrumental in the separation of the two species (4). This invasion may also have contributed to the rise of Lmb as a successful pathogen of *B. napus* due to the specific localisation of a number of candidate effector genes in TE-rich regions of the genome (4, 6). Differences in genomic organization between these two closely-related species could impact the underlying epigenomic landscape and have important consequences for fungal biology and pathogenicity. This could provide distinct strategies to regulate the expression of genes involved in stress response or pathogenicity, as it was shown in Lmb that histone modification H3K9me3 is involved in the repression of avirulence genes during axenic growth (33). To investigate this question, we here compared the genome-wide location of three different histone modifications that are typically associated with euchromatin or heterochromatin in these two closely-related phytopathogenic fungi. We found that differences in the epigenomic landscape of Lmb and Lml are in accordance with their genome organization. In Lmb, very large H3K9me3-domains are present, spanning large TE-rich regions, while such extremely large H3K9me3-domains are not observed in the Lml genome. Our findings corroborate previous epigenetic analyses of a few genes performed *in vitro*, pointing out that avirulence genes are located in heterochromatin, but also demonstrate that putative effector genes, independently of their expression pattern or their location in TE-rich or gene-rich regions,

417 are enriched with heterochromatin during axenic culture.

418

419 Although Lmb and Lml have distinct genome organisations, they share a common distribution of
420 histone modifications throughout their genome during axenic culture. Gene-rich regions are
421 enriched with H3K4me2 and H3K27me3, while TE-rich regions are associated with H3K9me3.
422 The proportion of H3K9me3 in a genome often reflects the TE content, as was described in *Z.*
423 *tritici* (43). In Lmb, having more than 30% of TE, 33% of the genome is associated with H3K9me3
424 while the genome of Lml, having a low TE content, shows a low enrichment in H3K9me3 (4% of
425 H3K9me3). Domains enriched with H3K4me2 and domains enriched with H3K9me3 are mutually
426 exclusive in the genomes of Lmb and Lml, as was shown in *Neurospora crassa*, *Fusarium*
427 *fujikuroi*, and *Z. tritici* (43, 60, 61, 62). H3K27me3 has been detected in most filamentous fungi
428 investigated so far, except in *Mucor*, *Rhizopus* or Aspergilli such as *Aspergillus nidulans* (63;
429 reviewed in 64). In sub-telomeric regions of Lmb, H3K9me3 and H3K27me3-domains overlap
430 over repetitive sequences, which is also the case in *N. crassa* or *Z. tritici* (43, 60, 61, 65). In the
431 genome of Lmb, TE-rich regions are enriched with H3K9me3 but, except for the sub-telomeric
432 regions, no enrichment in H3K27me3 was associated with TEs on chromosomal arms. This
433 contrasts with the organization of TE-rich regions in *Z. tritici*, which are enriched with both
434 heterochromatin modifications (43). The situation in Lmb is also different from that of *Fusarium*
435 *oxysporum* in which most TE sequences are embedded in H3K27me3-domains (66). We
436 confirmed that, as in most Eukaryotes, H3K4me2-domains are associated with expressed genes
437 while H3K9me3- and H3K27me3-domains are associated with silent genes. In Lmb, although the
438 locations of H3K4me2- and H3K27me3-domains do not overlap at a genome-wide scale, more

than 2,000 genes were found to be associated with both histone methylations. This is strikingly different to Lml, where only 300 genes were associated with both histone modifications, and *Z. tritici*, where 400 genes are embedded in such domains (35, 43). Bivalent domains are defined as chromatin regions associated with both repressive and permissive histone modifications (67). The large number of genes associated with H3K27me3 and H3K4me2 during axenic culture in Lmb might indicate a biological specificity of this species and the existence of bivalent domains, because these two modifications have antagonistic effects on gene expression (68). Altogether, our findings show that, despite differences in genomic organization between Lmb and Lml (and the other fungi in which epigenomic analyses were so far performed), the epigenomic landscape is overall conserved.

While H3K9me3 and H3K27me3 are signatures of heterochromatin, H3K9me3 is considered to be typical of constitutive heterochromatin, being associated with repeats and involved in genome stability, whereas H3K27me3 is considered to be associated with facultative heterochromatin that is easily reversed to a euchromatin state under certain abiotic and biotic stress conditions (69). However, dogmas regarding conventional definitions of facultative or constitutive heterochromatin seem to be challenged in fungi, or at least in the few plant pathogenic fungi in which epigenomic analyses have been performed. While the co-localization of H3K9me3 and TEs in the Lmb and Lml genomes is consistent with a constitutive heterochromatin state, the fact that H3K9me3-domains encompass genes that are expressed during interaction with oilseed rape suggests that these regions may correspond to a category of facultative heterochromatin in this species. Genes associated with H3K9me3 are almost all

461 located in the middle of repeated elements, in sub-telomeric areas, or very close to the edge of
462 regions enriched with repeated elements. Moreover, some of these genes, including the nine
463 cloned avirulence genes of Lmb which are located within AT-rich isochores (e.g., *AvrLm1* or
464 *AvLm6*; 17, 18) including subtelomeric regions (e.g. *AvrLm3* or AvrLm10; 24, 26), are highly
465 transcribed upon host infection (6). This finding, together with other studies, questions the
466 "constitutive" nature of heterochromatin associated with H3K9me3. In contrast, the location of
467 H3K27me3 in the genomes of Lmb and Lml supports its association with facultative
468 heterochromatin. Indeed, we found H3K27me3 associated with coding sequences and enriched
469 with genes encoding proteinaceous and metabolic effectors or proteins involved in stress
470 responses. Most of these genes are silenced during vegetative growth but induced during plant
471 infection. In fungi, recent analyses also highlighted a role for H3K27me3 in genome organization
472 and stability. For instance, the dispensable chromosomes of *Z. tritici* are twice as rich in TEs as
473 the core chromosomes, and whereas there is no significant enrichment in H3K9me3 on the
474 dispensable chromosomes, they are entirely covered by H3K27me3 (43). In *Z. tritici*, the loss of
475 H3K27me3 was found to increase the stability of some accessory chromosomes (70). In *Z. tritici*
476 and *N. crassa*, H3K27me3 is relocated towards normal constitutive heterochromatin (i.e.
477 H3K9me3-domains) under genotoxic stress, such as the loss of H3K9me3 after inactivation of
478 *KMT1* (70, 71). Altogether, these findings suggest that although H3K27me3 is an important
479 regulator of gene expression involved in development or response to various stresses, it also
480 plays a role in the maintenance of genome integrity. In Lmb and Lml, no particular association of
481 H3K27me3 with TEs was identified and the dispensable chromosome of Lmb is not enriched
482 with H3K27me3. The only association of H3K27me3 with constitutive chromatin was at the

chromosome ends of Lmb, where we found overlaps between H3K9me3 and H3K27me3. Inactivation of *KMT1* and *KMT6* would help investigate whether H3K27me3 could also be involved in genome stability and relocation of heterochromatin marks in Lmb and Lml.

The heterochromatin domains of Lmb and Lml are rich in species-specific genes, genes involved in stress responses and putative proteinaceous or metabolic effectors. This supports the view that chromatin remodelling mechanisms are an efficient way to rapidly modulate gene expression under stress conditions or during biotic interactions, although the dynamics of chromatin structure might not be the sole regulator of these complex biological processes (34, 72). This pattern is conserved in other plant-associated fungi, independently of their mode of interaction with their host (6, 32, 35, 43, 73, 74, 75, 76, 77). Even outside of TE-rich regions, heterochromatin is often found enriched with pathogenicity-related genes, whether they encode proteinaceous effectors or are involved in the production of secondary metabolites (e.g. 31, 32, 35, 43, 62, 66). Importantly, sets of genes up-regulated during host infection are found associated with heterochromatin *in vitro* (35, 66, 78). One of our initial postulates was that invasion of the *L. maculans* genome by TEs contributed to the rise of Lmb as a pathogen specialized on Brassicas with greater pathogenic abilities than the non-invaded sister species. While Lml has never been found to be able to infect *B. napus* under our experimental conditions or isolated from our experimental fields (M-H. Balesdent & T. Rouxel, unpublished data), previous work reported its ability to infect other crucifers (Petrie, 1969). Its isolation from ascocarps on stems of *Lepidium* sp. also suggests its infection strategy is similar to that of Lmb on *B. napus*. So far, all avirulence genes of Lmb, which can be recognized by the plant immune

505 system to set up defence reactions, are located in TE-rich regions and associated with H3K9me3.
506 In contrast, in both species we found conserved putative effector genes (either proteinaceous or
507 metabolic) harbored in similar H3K27me3 heterochromatin environments. Moreover, 'late'
508 effector genes are more conserved than avirulence genes between Lmb and Lml, and usually do
509 not show presence/absence polymorphisms in Lmb (27). The contrasting heterochromatic
510 environment (H3K9me3 vs. H3K27me3) for avirulence genes and 'late' effector genes reflects a
511 very different adaptive behaviour because effector genes that are expressed early, and likely to
512 be "recognised" by the plant surveillance machinery at the onset of penetration, are also those
513 which are subject to accelerated evolution under selection (6). This suggests that there may be a
514 selective advantage for the fungus to partition genes more likely to be recognised by the host
515 plant within H3K9me3-domains. Nevertheless, the location of putative pathogenicity genes,
516 including orthologues, in similar heterochromatin regions in the genomes of Lmb and Lml
517 suggests that basic pathogenicity programs are independent of genome invasion by TEs, and
518 points to the likewise importance of chromatin context on transcriptome shaping during
519 infection. Taken together, these data support our previous hypothesis that the localization of
520 effector genes in plastic genomic compartments is an efficient way to regulate the expression of
521 sets of genes scattered throughout the genome that are involved in similar biological processes
522 (34).
523
524 **Conclusions**
525 To the best of our knowledge, previous comparative analyses of histone modifications have been
526 performed in model organisms such as mouse (79) but none considered multiple histone

modifications (typical for both heterochromatin and euchromatin) in closely-related phytopathogenic fungi. Nothing is known about how differences in the location of these modifications influence pathogenesis. Comparative genomics has allowed analyses regarding the evolution of genes (notably proteinaceous effectors), the location of effector genes in genomes, or the diversity of effector repertoires in relation to host specialisation or fungal lifestyles. The role of the epigenome is increasingly recognized in plant-pathogenic fungi as an important regulator of genome structure (e.g. 70, 71, 80) and the expression of genes encoding effectors (e.g. 32, 33, 35). The next step is to exploit comparative epigenomics to better understand the role of the epigenomic landscape in adaptation to environmental changes, modulation of interactions with the holobiont, host adaptation and specialization.

Authors' contributions

Conceived, initiated and coordinated the project: JLS, TR, EHS, IF. Designed the experiments: JLS, EHS, IF. Performed the experiments: JLS. Analysis of the data: JLS, CC, EJG, NL. Interpretation of the data: JLS, TR, EHS, IF. Writing of the draft: JLS. Editing of the draft: JLS, CC, TR, EHS, IF.

Acknowledgments

Authors wish to thank all members of the "Effectors and Pathogenesis of *L. maculans*" and "Environmental Genomics" groups; M. Freitag and J. Grandaubert for fruitful discussions; R. O'Connell for the English proofreading of this paper.

Funding

549 J. L. Soyer was funded by a “Contrat Jeune Scientifique” grant from INRA. The “Effectors and
550 Pathogenesis of *L. maculans*” group benefits from the support of Saclay Plant Sciences-SPS
551 (ANR-17-EUR-0007). Research on fungal histone modifications in the group of E.H. Stukenbrock
552 is funded by the Max Planck Society, Germany. The funders had no role in study design, data
553 collection and interpretation, or the decision to submit the work for publication.

554

555 **Availability of data and material**

556 Omic data are available under the GEO accession number GSE150127.

557

558 **Ethics approval and consent to participate**

559 Not applicable.

560

561 **Consent for publication**

562 Not applicable.

563

564 **Conflict of interest**

565 None to declare.

566

567 **Competing interests**

568 Authors declare no competing interest.

569

570 **References**

571 1. Fisher MC, Hawkins NJ, Sanglard D, Gurr SJ. Worldwide emergence of resistance to antifungal
572 drugs challenges human health and food security. Science. 2018;360:739–42.
573 2. Rouxel T, Balesdent MH. Life, death and rebirth of avirulence effectors in a fungal pathogen of
574 Brassica crops, *Leptosphaeria maculans*. New Phytol. 2017;214:526–32.
575 3. Stukenbrock EH, Bataillon T, Dutheil JY, Hansen TT, Li R, Zala M, et al. The making of a new
576 pathogen: insights from comparative population genomics of the domesticated wheat pathogen
577 *Mycosphaerella graminicola* and its wild sister species. Genome Res. 2011;21:2157–66.
578 4. Grandaubert J, Lowe RG, Soyer JL, Schoch CL, Van de Wouw AP, Fudal I, et al. Transposable
579 element-assisted evolution and adaptation to host plant within the *Leptosphaeria maculans*-
580 *Leptosphaeria biglobosa* species complex of fungal pathogens. BMC Genomics. 2014;15:891.
581 5. Sánchez-Vallet A, Fouché S, Fudal I, Hartmann FE, Soyer JL, Tellier A, et al. The genome biology
582 of effector gene evolution in filamentous plant pathogens. Annu Rev Phytopathol. 2018;56:21–
583 40.
584 6. Rouxel T, Grandaubert J, Hane JK, Hoede C, van de Wouw AP, Couloux A, et al. Effector
585 diversification within compartments of the Leptosphaeria maculans genome affected by Repeat-
586 Induced Point mutations. Nat Commun. 2011;2:202.
587 7. Ohm RA, Feau N, Henrissat B, Schoch CL, Horwitz BA, Barry KW, et al. Diverse lifestyles and
588 strategies of plant pathogenesis encoded in the genomes of eighteen Dothideomycetes fungi.
589 PLoS Pathog. 2012;8:e1003037.
590 8. Croll D, McDonald BA. The accessory genome as a cradle for adaptive evolution in pathogens.
591 PLoS Pathog. 2012;8:e1002608.
592 9. de Jonge R, Bolton MD, Kombrink A, van den Berg GC, Yadeta KA, Thomma BP. Extensive

593 chromosomal reshuffling drives evolution of virulence in an asexual pathogen. Genome Res.
594 2013;23:1271–82.
595 10. Lo Presti L, Lanver D, Schweizer G, Tanaka S, Liang L, Tollot M, et al. Fungal effectors and
596 plant susceptibility. Annu Rev Plant Biol. 2015;66:513–45.
597 11. Collemare J, O'Connell R, Lebrun M-H. Nonproteinaceous effectors: the terra incognita of
598 plant-fungal interactions. New Phytol. 2019;223:590–6.
599 12. Rocafort M, Fudal I, Mesarich CH. Apoplastic effector proteins of plant-associated fungi and
600 oomycetes. Curr Opin Plant Biol. 2020;56:9–19.
601 13. Stergiopoulos I, De Kock MJ, Lindhout P, De Wit PJ. Allelic variation in the effector genes of
602 the tomato pathogen *Cladosporium fulvum* reveals different modes of adaptive evolution. Mol
603 Plant Microbe Interact. 2007;20:1271–83.
604 14. Chuma I, Isobe C, Hotta Y, Ibaragi K, Futamata N, Kusaba M, et al. Multiple translocation of
605 the *AVR-Pita* effector gene among chromosomes of the rice blast fungus *Magnaporthe oryzae*
606 and related species. PLoS Pathog. 2011;7:e1002147.
607 15. Jones JD, Dangl JL. The plant immune system. Nature. 2006;444:323–9.
608 16. Rouxel T, Balesdent MH. The stem canker (blackleg) fungus, *Leptosphaeria maculans*, enters
609 the genomic era. Mol Plant Pathol. 2005;6:225–41.
610 17. Gout L, Fudal I, Kuhn M-L, Blaise F, Eckert M, Cattolico L, et al. Lost in the middle of nowhere:
611 the *AvrLm1* avirulence gene of the Dothideomycete *Leptosphaeria maculans*. Mol Microbiol.
612 2006;60:67–80.
613 18. Fudal I, Ross S, Gout L, Blaise F, Kuhn ML, Eckert MR, et al. Heterochromatin-like regions as
614 ecological niches for avirulence genes in the *Leptosphaeria maculans* genome: map-based

615 cloning of *AvrLm6*. Mol Plant Microbe Interact. 2007;20:459–70.
616 19. Parlange F, Daverdin G, Fudal I, Kuhn M-L, Balesdent M-H, Blaise F, et al. *Leptosphaeria*
617 *maculans* avirulence gene *AvrLm4-7* confers a dual recognition specificity by the *Rlm4* and *Rlm7*
618 resistance genes of oilseed rape, and circumvents Rlm4-mediated recognition through a single
619 amino acid change. Mol Microbiol. 2009;71:851–63.
620 20. Balesdent M-H, Fudal I, Ollivier B, Bally P, Grandaubert J, Eber F, et al. The dispensable
621 chromosome of *Leptosphaeria maculans* shelters an effector gene conferring avirulence towards
622 *Brassica rapa*. New Phytol. 2013;198:887–898.
623 21. Van de Wouw AP, Lowe RG, Elliott CE, Dubois DJ, Howlett BJ. An avirulence gene, *AvrLmJ1*,
624 from the blackleg fungus, *Leptosphaeria maculans*, confers avirulence to *Brassica juncea*
625 cultivars. Mol Plant Pathol. 2014;15:523–30.
626 22. Ghanbarnia K, Fudal I, Larkan NJ, Links MG, Balesdent M-H, Profotova B, et al. Rapid
627 identification of the *Leptosphaeria maculans* Avirulence gene *AvrLm2* using an intraspecific
628 comparative genomics approach. Mol Plant Pathol. 2015;16:699–709.
629 23. Ghanbarnia K, Ma L, Larkan NJ, Haddadi P, Fernando WGD, Borhan MH. *Leptosphaeria*
630 *maculans* AvrLm9: a new player in the game of hide and seek with AvrLm4-7. Mol Plant Pathol.
631 2018;19: 1754–64.
632 24. Plissonneau C, Daverdin G, Ollivier B, Blaise F, Degrave A, Fudal I, et al. A game of hide and
633 seek between avirulence genes *AvrLm4-7* and *AvrLm3* in *Leptosphaeria maculans*. New Phytol.
634 2016;209:1613–24.
635 25. Plissonneau C, Rouxel T, Chèvre A-M, Van De Wouw AP, Balesdent M-H. One gene-one name:
636 the *AvrLmJ1* avirulence gene of *Leptosphaeria maculans* is *AvrLm5*. Mol Plant Pathol.

637 2018;19:1012–16.
638 26. Petit-Houdenot Y, Degrave A, Meyer M, Blaise F, Ollivier B, Marais C-L, et al. A two genes - for
639 - one gene interaction between *Leptosphaeria maculans* and *Brassica napus*. New Phytol.
640 2019;223:397–411.
641 27. Gervais J, Plissonneau C, Linglin J, Meyer M, Labadie K, Cruaud C, et al. Different waves of
642 effector genes with contrasted genomic location are expressed by *Leptosphaeria maculans*
643 during cotyledon and stem colonization of oilseed rape. Mol Plant Pathol. 2017;18:1113–26.
644 28. Zhao Y, Garcia BA. Comprehensive catalog of currently documented histone modifications.
645 Cold Spring Harb Perspect Biol. 2015;7:a025064.
646 29. Gomes MV, Pelosi GG. Epigenetic vulnerability and the environmental influence on health.
647 Exp Biol Med (Maywood). 2013;238:859–65.
648 30. Zogli P, Libault M. Plant response to biotic stress: Is there a common epigenetic response
649 during plant-pathogenic and symbiotic interactions? Plant Sci. 2017;263:89–93.
650 31. Connolly LR, Smith KM, Freitag M. The *Fusarium graminearum* histone H3K27
651 methyltransferase KMT6 regulates development and expression of secondary metabolite gene
652 clusters. PLoS Genet. 2013;9:e1003916.
653 32. Chujo T, Scott B. Histone H3K9 and H3K27 methylation regulates fungal alkaloid biosynthesis
654 in a fungal endophyte-plant symbiosis: K9 and K27 methylation regulates symbiosis. Mol
655 Microbiol. 2014;92:413–34.
656 33. Soyer JL, El Ghalid M, Glaser N, Ollivier B, Linglin J, Grandaubert J, et al. Epigenetic control of
657 effector gene expression in the plant pathogenic fungus *Leptosphaeria maculans*. PLoS Genet.
658 2014;10:e1004227.

659 34. Soyer JL, Rouxel T, Fudal I. A. Chromatin-based control of effector gene expression in plant-
660 associated fungi. Curr Opin Plant Biol. 2015;26:51–6.
661 35. Soyer JL, Grandaubert J, Haueisen J, Schotanus K, Stukenbrock EH. *In planta* chromatin
662 immunoprecipitation in *Zymoseptoria tritici* reveals chromatin-based regulation of putative
663 effector gene expression. 2019. Preprint at bioRxiv. https://doi.org/10.1101/544627
664 36. Daverdin G, Rouxel T, Gout L, Aubertot JN, Fudal I, Meyer M, et al. Genome structure and
665 reproductive behaviour influence the evolutionary potential of a fungal phytopathogen. PLoS
666 Pathog. 2012 ;8:1003020.
667 37. Dutreux F, Da Silva C, d'Agata L, Couloux A, Gay EJ, Istace B, et al. De novo assembly and
668 annotation of three *Leptosphaeria* genomes using Oxford Nanopore MinION sequencing. Sci
669 Data; 2018;5:180235.
670 38. Petrie GA. Variability in *Leptosphaeria maculans* (Desm.) Ces. et De Not., the cause of
671 blackleg of rape. 1969. PhD thesis, University of Saskatchewan (215 pp.).
672 39. Zhang Z, Wen J, Li J, Ma X, Yu Y, Tan X, et al. The evolution of genomic and epigenomic
673 features in two Pleurotus fungi. Sci Rep. 2018;8:8313.
674 40. Feurtey A, Lorrain C, Croll D, Eschenbrenner C, Freitag M, Habig M, et al. Genome
675 compartmentalization predates species divergence in the plant pathogen genus *Zymoseptoria.*
676 2019. Preprint at bioRXiv. https://doi.org/10.1101/864561
677 41. Ansan-Melayah D, Balesdent M-H, Buee M, Rouxel T. Genetic characterization of *AvrLm1*, the
678 first avirulence gene of *Leptosphaeria maculans*. Phytopathology. 1995;85:1525–9.
679 42. Soyer JL, Möller M, Schotanus K, Connolly LR, Galazka JM, Freitag M, et al. Chromatin
680 analyses of *Zymoseptoria tritici*: Methods for chromatin immunoprecipitation followed by high-

681 throughput sequencing (ChIP-seq). Fungal Genet Biol. 2015;79:63–70.
682 43. Schotanus K, Soyer JL, Connolly LR, Grandaubert J, Happel P, Smith KM, et al. Histone
683 modifications rather than the novel regional centromeres of *Zymoseptoria tritici* distinguish core
684 and accessory chromosomes. Epigenetics Chromatin. 2015;8:41.
685 44. Langmead B, Salzberg SL. Fast gapped-read alignment with Bowtie 2. Nat Methods.
686 2012;9:357–9.
687 45. Song Q, Smith AD. Identifying dispersed epigenomic domains from ChIP-Seq data.
688 Bioinformatics. 2011;27:870–1.
689 46. Thorvaldsdóttir H, Robinson JT, Mesirov JP. Integrative Genomics Viewer (IGV): high-
690 performance genomics data visualization and exploration. Brief Bioinform. 2013;14:178–92.
691 47. Bolger AM, Lohse M, Usadel B. Trimmomatic: a flexible trimmer for Illumina sequence data.
692 Bioinformatics. 2014;30:2114–20.
693 48. Dobin A, Gingeras TR. Mapping RNA-seq reads with STAR. Current Protoc Bioinformatics.
694 2015;3, 51:11.14.1-11.14.19.
695 49. Robinson MD, McCarthy DJ, Smyth GK. edgeR: a Bioconductor package for differential
696 expression analysis of digital gene expression data. Bioinformatics. 2010;26:139–40.
697 50. Emms DM, Kelly S. OrthoFinder: solving fundamental biases in whole genome comparisons
698 dramatically improves orthogroup inference accuracy. Genome Biol. 2015;16:157.
699 51. Petersen TN, Brunak S, von Heijne G, Nielsen H. SignalP 4.0: discriminating signal peptides
700 from transmembrane regions. Nat Methods. 2011;8:785–6.
701 52. Almagro Armenteros JJ, Salvatore M, Emanuelsson O, Winther O, von Heijne G, Elofsson A, et
702 al. Detecting sequence signals in targeting peptides using deep learning. Life Sci Alliance.

703 2019;2:5.
704 53. Sperschneider J, Gardiner DM, Dodds PN, Tini F, Covarelli L, Singh KB, et al. EffectorP:
705 predicting fungal effector proteins from secretomes using machine learning. New phytol.
706 2016;210:743–61.
707 54. Shannon P, Markiel A, Ozier O, Baliga NS, Wang JT, Ramage D, et al. Cytoscape: a software
708 environment for integrated models of biomolecular interaction networks. Genome Res.
709 2003;13:2498–504.
710 55. Leclair S, Ansan-Melayah D, Rouxel T, Balesdent M-H. Meiotic behaviour of the
711 minichromosome in the phytopathogenic ascomycete *Leptosphaeria maculans*. Curr Genet.
712 1996;30:541–8.
713 56. Darma R, Lutz A, Elliott CE, Idnurm A. Identification of a gene cluster for the synthesis of the
714 plant hormone abscisic acid in the plant pathogen *Leptosphaeria maculans*. Fungal Genet Biol.
715 2019;130:62–71.
716 57. Elliott CE, Callahan DL, Schwenk D, Nett M, Hoffmeister D, Howlett BJ. A gene cluster
717 responsible for biosynthesis of phomenoic acid in the plant pathogenic fungus, *Leptosphaeria*
718 *maculans*. Fungal Genet Biol. 2013;53:50–8.
719 58. Gardiner DM, Cozijnsen AJ, Wilson LM, Pedras MS, Howlett BJ. The sirodesmin biosynthetic
720 gene cluster of the plant pathogenic fungus *Leptosphaeria maculans*. Mol Microbiol.
721 2004;53:1307–18.
722 59. Elliott CE, Gardiner DM, Thomas G, Cozijnsen A, Van De Wouw A, Howlett BJ. Production of
723 the toxin sirodesmin PL by *Leptosphaeria maculans* during infection of *Brassica napus*. Mol Plant
724 Pathol. 2007;8:791–802.

60. Smith KM, Kothe GO, Matsen CB, Khlafallah TK, Adhvaryu KK, Hemphill M, et al. The fungus *Neurospora crassa* displays telomeric silencing mediated by multiple sirtuins and by methylation of histone H3 lysine 9. Epigenetics Chromatin. 2008;1:5.

61. Jamieson K, Rountree MR, Lewis ZA, Stajich JE, Selker EU. Regional control of histone H3 lysine 27 methylation in *Neurospora*. Proc Natl Acad Sci U S A. 2013;110:6027–32.

62. Wiemann P, Sieber CM, von Bargen KW, Studt L, Niehaus EM, Espino JJ, et al. Deciphering the cryptic genome: genome-wide analyses of the rice pathogen *Fusarium fujikuroi* reveal complex regulation of secondary metabolism and novel metabolites. PLoS Pathog. 2013;9:e1003475.

63. Gacek-Matthews A, Berger H, Sasaki T, Wittstein K, Gruber C, Lewis ZA, et al. KdmB, a Jumonji Histone H3 demethylase, regulates genome-wide H3K4 trimethylation and is required for normal induction of secondary metabolism in *Aspergillus nidulans*. PLoS Genet. 2016;12:e1006222.

64. Freitag M. Histone methylation by SET domain proteins in Fungi. Annu Rev Microbiol. 2017;71:413–39.

65. Jamieson K, McNaught KJ, Ormsby T, Leggett NA, Honda S, Selker EU. Telomere repeats induce domains of H3K27 methylation in *Neurospora*. Elife. 2018;7:e31216.

66. Fokkens L, Shahi S, Connolly LR, Stam R, Schmidt SM, Smith KM, et al. The multi-speed genome of *Fusarium oxysporum* reveals association of histone modifications with sequence divergence and footprints of past horizontal chromosome transfer events. 2018. Preprint at bioRXiv. https://doi.org/10.1101/465070

67. Bernstein BE, Mikkelsen TS, Xie X, Kamal M, Huebert DJ, Cuff J, et al. A bivalent chromatin structure marks key developmental genes in embryonic stem cells. Cell. 2006;125:315–26.

747 68. Harikumar A, Meshorer E. Chromatin remodeling and bivalent histone modifications in
748 embryonic stem cells. EMBO Rep. 2015;16:1609–19.
749 69. Grewal SI, Jia S. Heterochromatin revisited. Nat Rev Genet. 2007;8:35–46.
750 70. Möller M, Schotanus K, Soyer JL, Haueisen J, Happ K, Stralucke M, et al. Destabilization of
751 chromosome structure by histone H3 lysine 27 methylation. PLoS Genet. 2019;15:e1008093.
752 71. Basenko EY, Sasaki T, Ji L, Prybol CJ, Burckhardt RM, Schmitz RJ, et al. Genome-wide
753 redistribution of H3K27me3 is linked to genotoxic stress and defective growth. Proc Natl Acad Sci
754 U S A. 2015;112:E6339–48.
755 72. Tan KC, Oliver RP. Regulation of proteinaceous effector expression in phytopathogenic fungi.
756 PLoS Pathog. 2017;13:e1006241.
757 73. Ma LJ, van der Does HC, Borkovich KA, Coleman JJ, Daboussi MJ, Di Pietro A, et al.
758 Comparative genomics reveals mobile pathogenicity chromosomes in *Fusarium*. Nature.
759 2010 ;464:367–73.
760 74. Faino L, Seidl MF, Shi-Kunne X, Pauper M, van den Berg GC, Wittenberg AH, et al.
761 Transposons passively and actively contribute to evolution of the two-speed genome of a fungal
762 pathogen. Genome Res. 2016;26:1091–1100.
763 75. Vlaardingerbroek I, Beerens B, Schmidt SM, Cornelissen BJ, Rep M. Dispensable
764 chromosomes in *Fusarium oxysporum* f. sp. lycopersici. Mol Plant Pathol. 2016;17:1455–66.
765 76. Dallery JF, Lapalu N, Zampounis A, Pigné S, Luyten I, Amselem J, et al. Gapless genome
766 assembly of *Colletotrichum higginsianum* reveals chromosome structure and association of
767 transposable elements with secondary metabolite gene clusters. BMC Genomics. 2017;18:667.
768 77. Krishnan P, Meile L, Plissonneau C, Ma X, Hartmann FE, Croll D, et al. Transposable element

769 insertions shape gene regulation and melanin production in a fungal pathogen of wheat. BMC
770 Biol. 2018;16:78.
771 78. Haueisen J, Möller M, Eschenbrenner CJ, Grandaubert J, Seybold H, Adamiak H, et al. Highly
772 flexible infection programs in a specialized wheat pathogen. Ecol Evol. 2018;9:275–94.
773 79. Mikkelsen TS, Xu Z, Zhang X, Wang L, Gimble JM, Lander ES, et al. Comparative epigenomic
774 analysis of murine and human adipogenesis. Cell. 2010;143:156–69.
775 80. Möller M, Habig M, Lorrain C, Feurtey A, Haueisen J, Fagundes WC, et al. Recent loss of the
776 Dim2 cytosine DNA methyltransferase impacts mutation rate and evolution in a fungal plant
777 pathogen. 2020. Preprint at bioRXiv. https://doi.org/10.1101/2020.03.27.012203
778
779 **Figure legends**
780 **Figure 1. Size of the histone domains in the genomes of *Leptosphaeria maculans* 'brassicae'**
781 **and *L. maculans* 'lepidii'**. Log2 of the size of the domains was estimated based on the
782 coordinates of the location of the domains, identified using RSEG (45). Blue: H3K4me2; Purple:
783 H3K9me3; Orange: H3K27me3; Lmb: *L. maculans* 'brassicae'; Lml: *L. maculans* 'lepidii'.
784
785 **Figure 2. Genome of *Leptosphaeria maculans* 'brassicae' harbors large TE-rich, H3K9me3-**
786 **domains compared to *Leptosphaeria maculans* 'lepidii'.** Example of SuperContig 2 of Lmb and
787 Scaffold 1 of Lml. ChIP-seq was performed with antibodies targeting H3K4me2 (cyan), H3K9me3
788 (purple) or H3K27me3 (orange); rectangles indicate location of significantly enriched domains
789 identified using RSEG (45). Blue: location of CDS; red: location of transposable elements; Lmb: *L.*
790 *maculans* 'brassicae'; Lml: *L. maculans* 'lepidii'. Genes encoding proteinaceous effectors are

791 indicated with a red square.

792

793 **Figure 3. Coverage of different genome features in the genomes of *L. maculans* 'brassicae' and**
794 ***L. maculans* 'lepidii'.** A. SuperContig 2 of Lmb; B. SC 19, i.e. dispensable chromosome, of Lmb; C.
795 SC 1 of Lml. SC2 of Lmb and SC1 of Lml are syntenic (4). Coverage of the genome features and
796 histone modification domains, as identified in axenic cultures, were analysed in 10 kb sliding
797 windows in the genomes of Lmb and Lml. Lmb, *L. maculans* 'brassicae'; Lml, *L. maculans* 'lepidii';
798 CDS, Coding Sequences; TE, Transposable Elements; SC, Super Contig.

799

800 **Figure 4. Number of genes associated with histone modifications in *Leptosphaeria maculans***
801 **'brassicae' and *L. maculans* 'lepidii'.** A. *L. maculans* 'brassicae', Lmb and B. *L. maculans* 'lepidii',
802 Lml. Locations of histone modifications in the genomes of Lmb and Lml were identified using
803 RSEG (45). Blue: H3K4me2; Purple: H3K9me3; Orange: H3K27me3. Genes were considered as
804 associated with any of the histone modifications when at least one bp of the gene was found
805 within the borders of the domain.

806

807 **Figure 5. Genes associated with heterochromatin are less expressed than genes associated**
808 **with euchromatin in *L. maculans* 'brassicae' and *L. maculans* 'lepidii'.** A. *L. maculans*
809 'brassicae'; B. *L. maculans* 'lepidii'. Location of histone modifications in the genomes of Lmb and
810 Lml were identified using RSEG (45), during axenic culture. RNA-seq was performed from Lmb or
811 Lml grown one week in FRIES media. Blue: H3K4me2; Purple: H3K9me3; Orange: H3K27me3.

Table 3. Number of proteinaceous effector genes located in different genomic compartments in *L. maculans* 'brassicae' and *L. maculans* 'lepidii'

	L. maculans 'brassicae'							*L. maculans* 'lepidii'						
		effector-genes			specific effector-genes				effector-genes			specific effector-genes		
	number of genes	number	proportion	*P value* [c]	number	proportion	*P value* [c]	number of genes	number	proportion	*P value* [c]	number	proportion	*P value* [c]
genome	13,047	1,080	$8.2.10^{-2}$	-	806	$6.2.10^{-2}$	-	11,272	892	$7.9.10^{-2}$	-	618	$5.5.10^{-2}$	-
TE-associated genes[a]	2,478	289	$1.2.10^{-1}$	$9.6.10^{-16}$	210	$8.5.10^{-2}$	$2.2.10^{-6}$	641	79	$1.2.10^{-1}$	$3.5.10^{-5}$	66	1.10^{-1}	1.10^{-7}
H3K4me2-domains[b]	7,373	433	$5.8.10^{-2}$	$6.7.10^{-14}$	319	$4.3.10^{-2}$	$2.6.10^{-11}$	6,065	266	$4.4.10^{-2}$	$2.2.10^{-16}$	163	$2.7.10^{-2}$	$2.2.10^{-16}$
H3K9me3-domains[b]	104	38	$3.6.10^{-1}$	$2.2.10^{-16}$	35	$3.4.10^{-1}$	$2.2.10^{-16}$	70	14	2.10^{-1}	$1.8.10^{-4}$	14	2.10^{-1}	$1.3.10^{-7}$
H3K27me3-domains[b]	2,020	286	$1.4.10^{-1}$	$2.2.10^{-16}$	200	$9.9.10^{-2}$	$5.3.10^{-12}$	1,501	217	$1.45.10^{-1}$	$2.2.10^{-16}$	152	1.10^{-1}	$3.8.10^{-15}$
H3K9+H3K27me3-domains[b]	101	24	$2.4.10^{-1}$	$1.6.10^{-8}$	16	$1.6.10^{-1}$	$5.9.10^{-5}$	58	18	$3.1.10^{-1}$	$6.9.10^{-11}$	14	$2.4.10^{-1}$	$4.8.10^{-10}$

[a]Genes located up to 2 kb upstream or downstream of a transposable element sequence;

[b]Genes located in a H3K4me2-, H3K9me3-, H3K27me3- or H3K9me3/H3K27me3-domain *in vitro* ;

[c]A X^2 test was applied to compare proportion of effector genes in the genome and in the genomic compartment analysed.

Additional figure legends

Additional figure 1. Correlation analysis of the location of genes, transposable elements and domains enriched for H3K4me2, H3K9me3 and H3K27me3 in the genomes of A. *Leptosphaeria maculans* 'brassicae'; B. *Leptosphaeria maculans* 'lepidii'. Regions significantly enriched for any of the three histone modifications analysed were identified through ChIP-seq performed during axenic culture; correlation analyses were performed using a Kendall's *T* (see Materials and Methods). K4: H3K4me2; K9: H3K9me3; K27: H3K27me3; CDS: Coding sequences; TE: Transposable Elements.

Additional table legends

Additional table 1. Statistics of ChIP-seq and RNA-seq datasets and alignments. Table shows the number of reads used for the alignment, the number of reads mapping only at one location, the number of reads aligned more than once and the unmapped reads against the genome of *L. maculans* 'brassicae' (Lmb; 37) or *L. maculans* 'lepidii' (Lml; 4).

Additional table 2. Correlation analysis between the different ChIP experiments generated with antibodies targeting histone modifications H3K4me2, H3K9me3 and H3K27me3 in *L. maculans* 'brassicae', during *in vitro* growth. Correlation analyses were performed to analyse location of the significantly enriched domains, identified using RSEG (45), from the three different biological replicates generated and analyzed separately. A Kendall's *T* correlation test was performed using R.

Additional table 3. Correlation analysis between the different ChIP experiments generated with antibodies targeting histone modifications H3K4me2, H3K9me3 and H3K27me3 in *L. maculans* 'lepidii', during *in vitro* growth.

Correlation analyses were performed to analyse location of the significantly enriched domains, identified using RSEG (45), from the three different biological replicates generated and analyzed separately. A Kendall's *T* correlation test was performed using R.

Additional table 4. Coverage of histone modifications H3K4me2, H3K9me3 and H3K27me3 in the genome of *Leptosphaeria maculans* 'brassicae'.

[a]Genome as published in Dutreux *et al*. (37)

[b]Location of H3K4me2, H3K9me3 and H3K27me3 was determined through ChIP-seq analysis, *in vitro*, and regions significantly enriched for any of the modifications was identified using RSEG (45).

Additional table 5. Coverage of histone modifications H3K4me2, H3K9me3 and H3K27me3 in the genome of *L. maculans* 'lepidii'.

[a]Genome as published in Grandaubert *et al*. (4)

[b]Location of H3K4me2, H3K9me3 and H3K27me3 was determined through ChIP-seq analysis, in vitro, and regions significantly enriched for any of the modifications was identified using RSEG (45).

Additional table 6. GO categories enriched in genes associated with H3K4me2 during axenic culture of *L. maculans* 'brassicae'. GO annotation of the Lmb genes were retrieved from Dutreux *et al*. (37). Analysis of GO enrichment among the genes associated with H3K4me2 during axenic culture of Lmb was performed using Cytoscape (Shannon *et al*., 2003).

Additional table 7. GO categories enriched in genes associated with H3K4me2 during axenic culture of *L. maculans* 'lepidii'. GO annotation of the Lml genes were retrieved from Grandaubert *et al*. (4). Analysis of GO enrichment among the genes associated with H3K4me2 during axenic culture of Lml was performed using Cytoscape (54).

Additional table 8. GO categories enriched in genes associated with H3K27me3 during axenic culture of *L. maculans* 'brassicae'. GO annotation of the Lmb genes were retrieved from Dutreux *et al*. (37). Analysis of GO enrichment among the genes associated with H3K27me3 during axenic culture of Lmb was performed using Cytoscape (54).

Additional table 9. GO categories enriched in genes associated with H3K27me3 during axenic culture of *L. maculans* 'lepidii'. GO annotation of the Lml genes were retrieved from Grandaubert *et al*. (4). Analysis of GO enrichment among the genes associated with H3K27me3 during axenic culture of Lml was performed using Cytoscape (54).

Additional table 10. Location of (putative) metabolic effector in *L. maculans* 'brassicae' and *L. maculans* 'lepidii' genomic compartments.

879 [a]Genes located up to 2 kb upstream or downstream of a transposable element sequence;

880 [b]Genes with RPKM≥ 2;

881 [c]Genes located in a H3K4me2-, H3K9me3-, H3K27me3- or H3K4me2/H3K27me3-domain *in vitro*;

882 K4: H3K4me2; K9: H3K9me3; K27:H3K27me3.

883

Figures

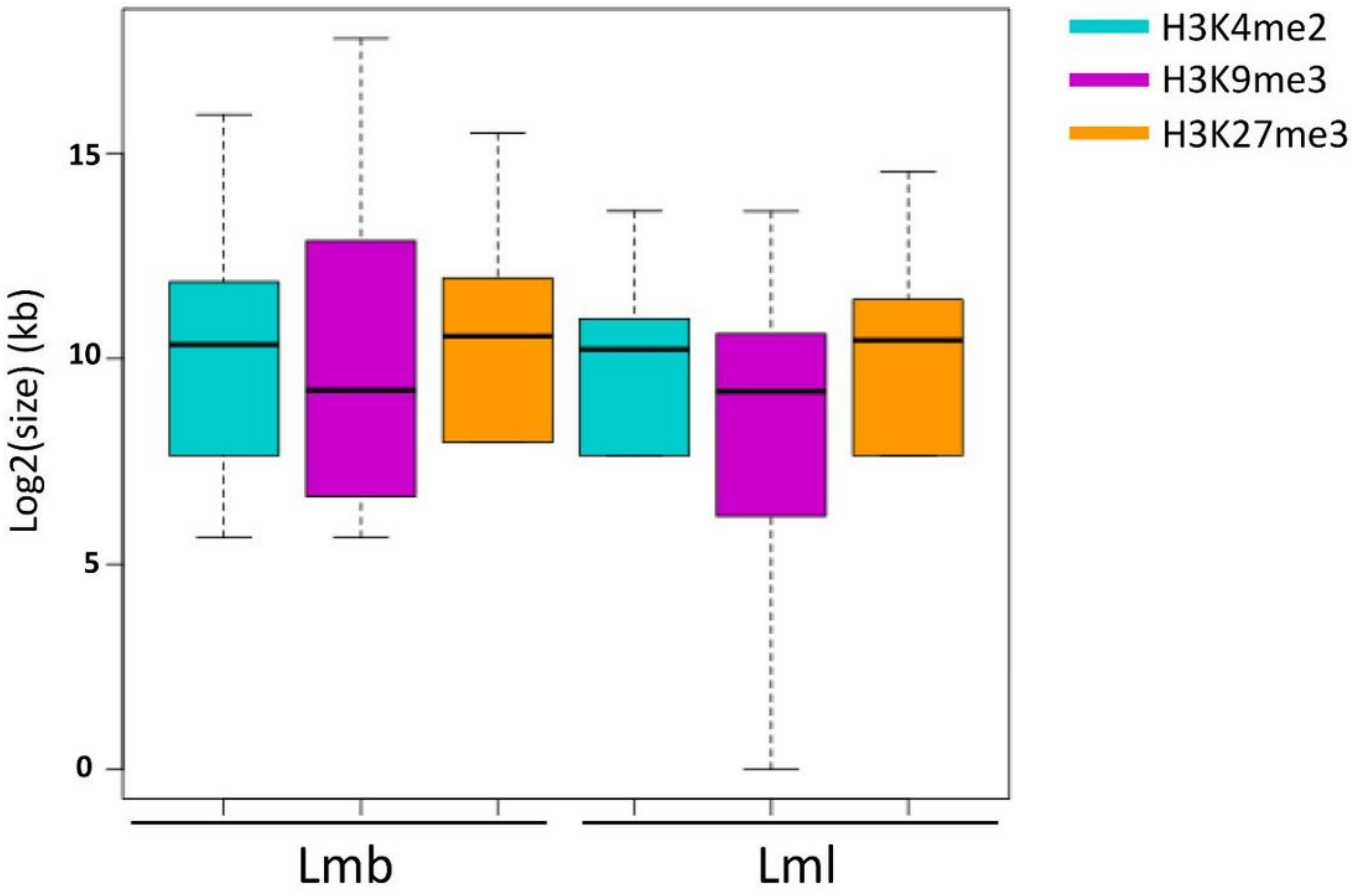

Figure 1

Size of the histone domains in the genomes of Leptosphaeria maculans ‘brassicae’ and L. maculans ‘lepidii’. Log2 of the size of the domains was estimated based on the coordinates of the location of the domains, identified using RSEG (45). Blue: H3K4me2; Purple: H3K9me3; Orange: H3K27me3; Lmb: L. maculans ‘brassicae’; Lml: L. maculans ‘lepidii’.

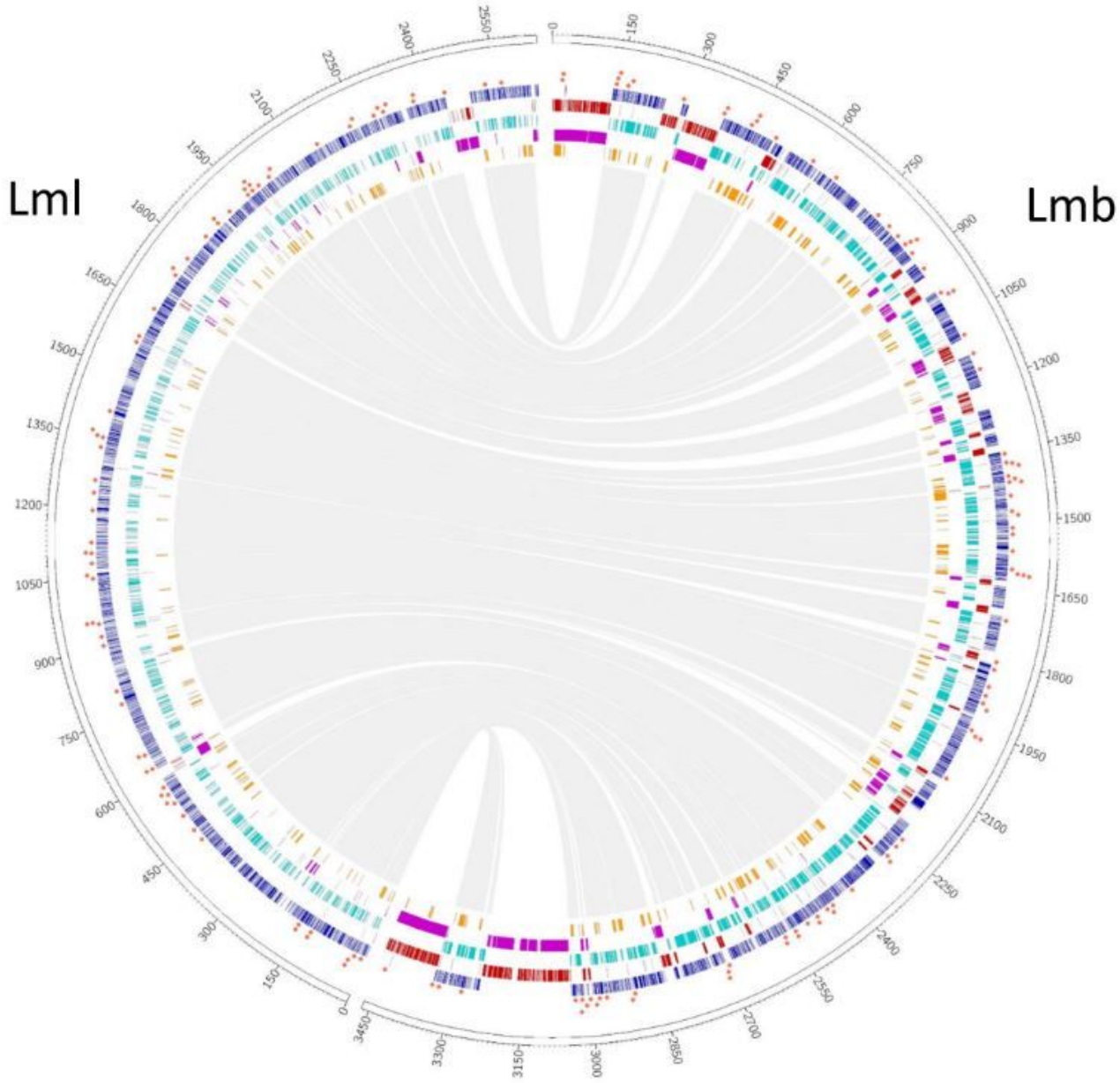

Figure 2

Genome of Leptosphaeria maculans ‘brassicae’ harbors large TE-rich, H3K9me3-domains compared to Leptosphaeria maculans ‘lepidii’. Example of SuperContig 2 of Lmb and Scaffold 1 of Lml. ChIP-seq was performed with antibodies targeting H3K4me2 (cyan), H3K9me3 (purple) or H3K27me3 (orange); rectangles indicate location of significantly enriched domains identified using RSEG (45). Blue: location

of CDS; red: location of transposable elements; Lmb: L. maculans ‘brassicae’; Lml: L. maculans ‘lepidii’. Genes encoding proteinaceous effectors are indicated with a red square.

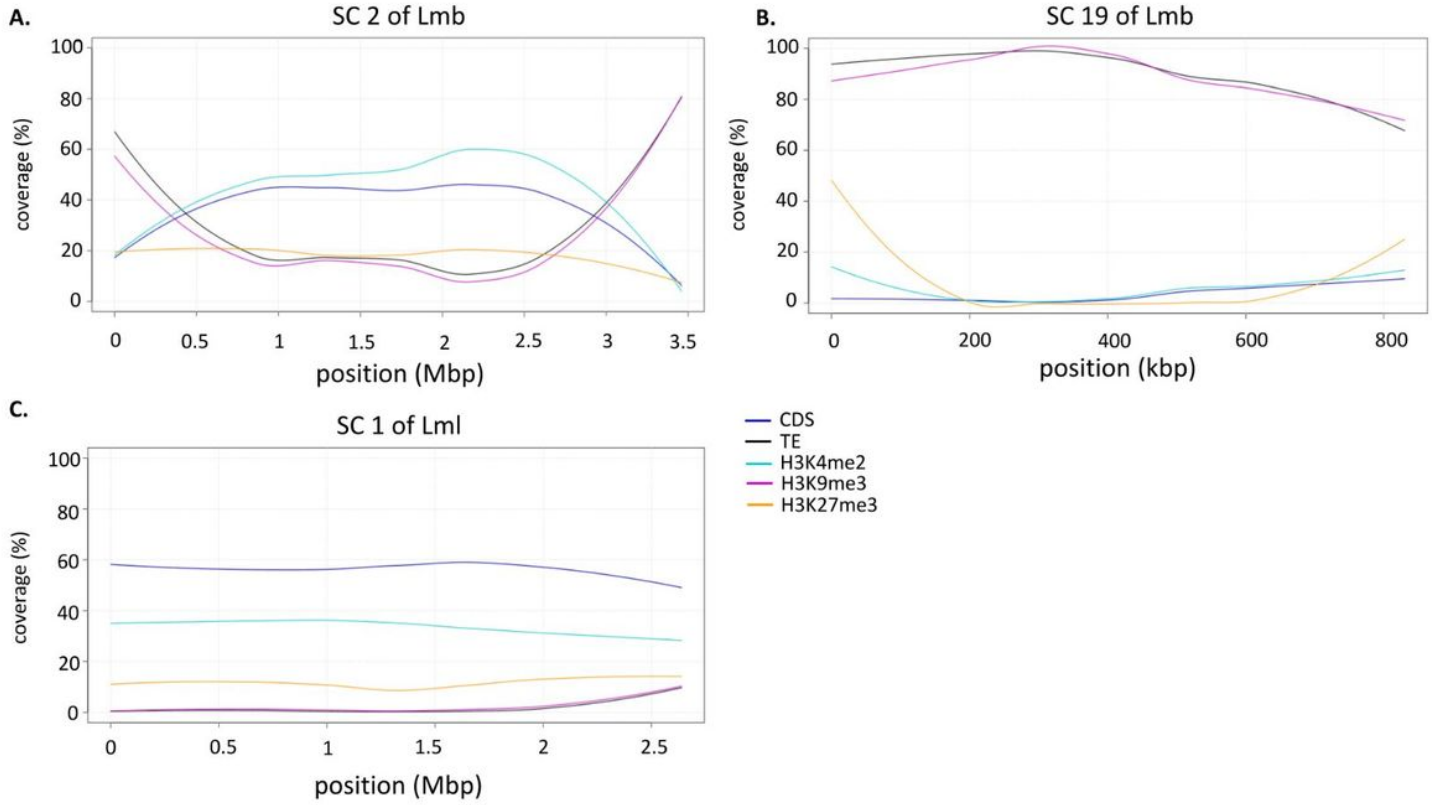

Figure 3

Coverage of different genome features in the genomes of L. maculans ‘brassicae’ and L. maculans ‘lepidii’. A. SuperContig 2 of Lmb; B. SC 19, i.e. dispensable chromosome, of Lmb; C. SC 1 of Lml. SC2 of Lmb and SC1 of Lml are syntenic (4). Coverage of the genome features and histone modification domains, as identified in axenic cultures, were analysed in 10 kb sliding windows in the genomes of Lmb and Lml. Lmb, L. maculans ‘brassicae’; Lml, L. maculans ‘lepidii’; CDS, Coding Sequences; TE, Transposable Elements; SC, Super Contig.

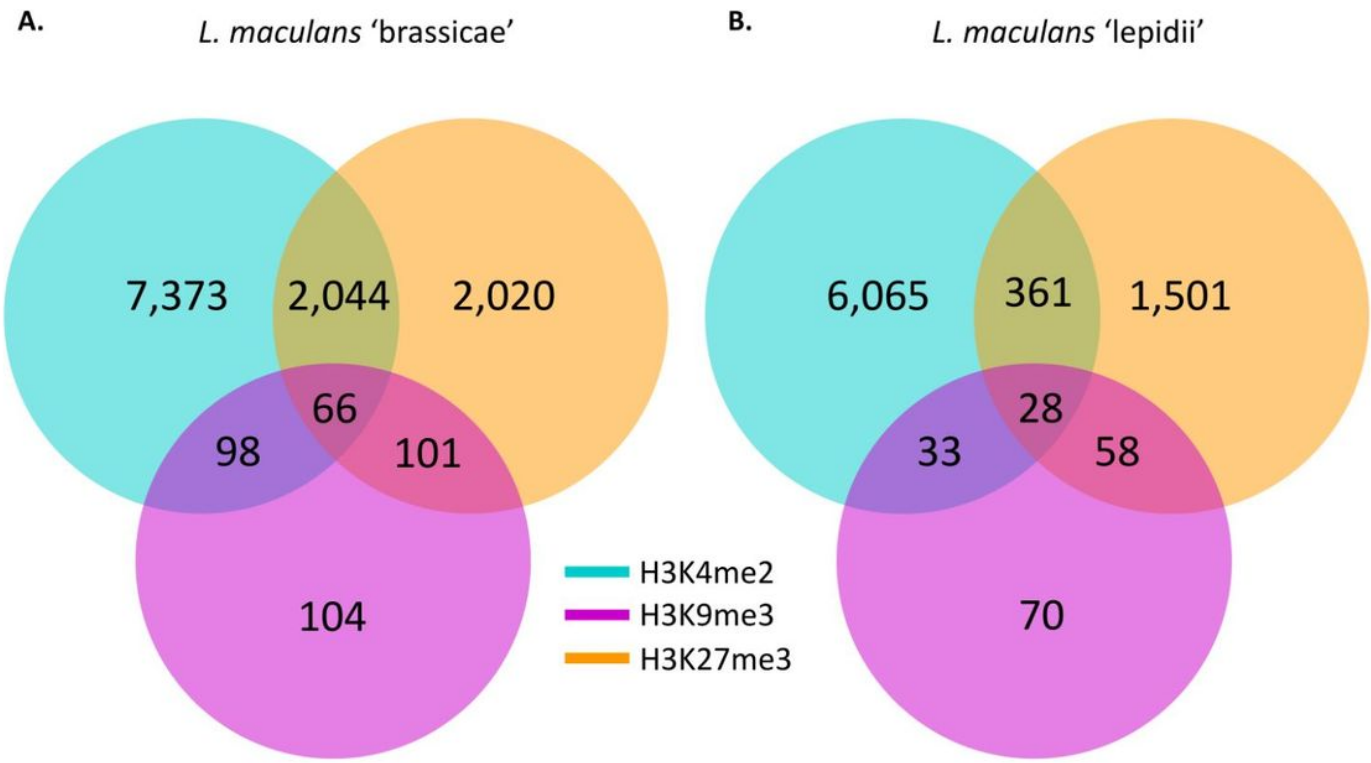

Figure 4

Number of genes associated with histone modifications in Leptosphaeria maculans 'brassicae' and L. maculans 'lepidii'. A. L. maculans 'brassicae', Lmb and B. L. maculans 'lepidii', Lml. Locations of histone modifications in the genomes of Lmb and Lml were identified using RSEG (45). Blue: H3K4me2; Purple: H3K9me3; Orange: H3K27me3. Genes were considered as associated with any of the histone modifications when at least one bp of the gene was found within the borders of the domain.

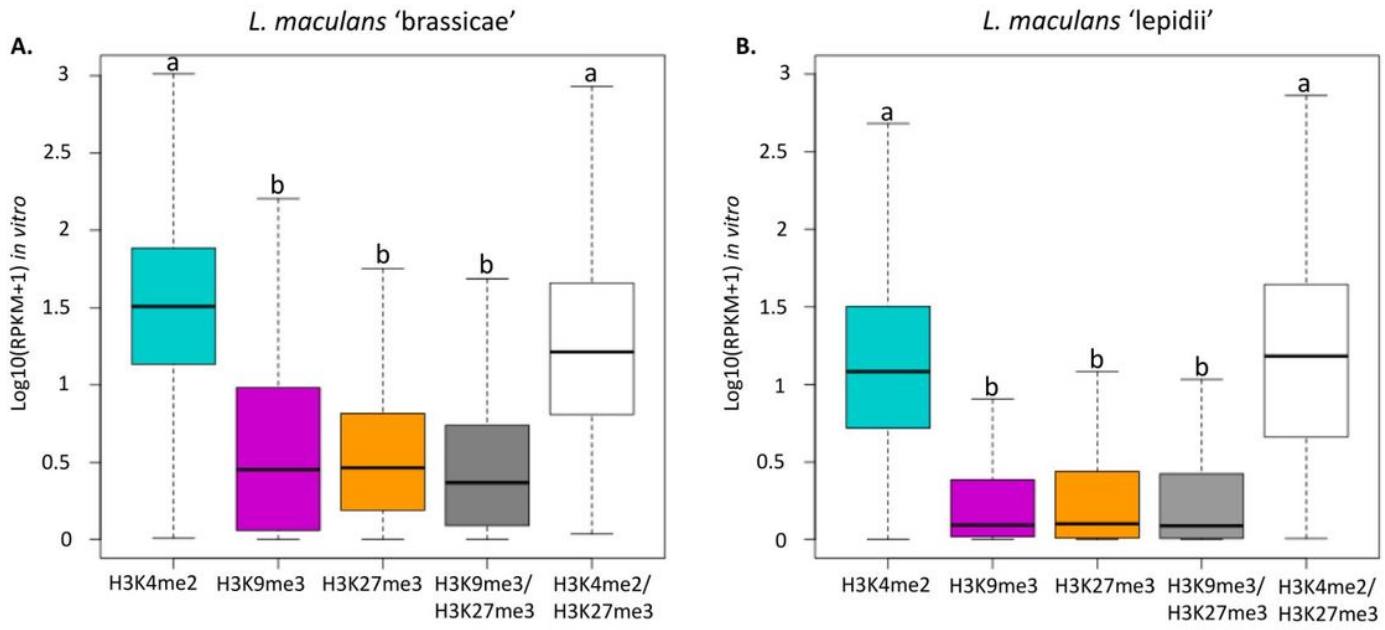

Figure 5

Genes associated with heterochromatin are less expressed than genes associated with euchromatin in L. maculans 'brassicae' and L. maculans 'lepidii'. A. L. maculans 'brassicae'; B. L. maculans 'lepidii'. Location of histone modifications in the genomes of Lmb and Lml were identified using RSEG (45), during axenic culture. RNA-seq was performed from Lmb or Lml grown one week in FRIES media. Blue: H3K4me2; Purple: H3K9me3; Orange: H3K27me3.

Supplementary Files

This is a list of supplementary files associated with this preprint. Click to download.

- Additionaltable10.pdf
- Additionaltable9.pdf
- Additionaltable8.pdf
- Additionaltable7.pdf
- Additionaltable6.pdf
- Additionaltable5.pdf
- Additionaltable4.pdf
- Additionaltable3.pdf
- Additionaltable2.pdf
- Additionaltable1.pdf

- FigureS1.tiff